AN ELECTRON–NUCLEUS COLLIDER DESIGN STUDY (ENC)

K. Blasche, J. Struckmeier,
GSI, Planckstrasse 1, 64291 Darmstadt, Germany
N.S. Dikansky, Yu.I. Eidelman, B.I. Grishanov, V.V. Parkhomchuk,
D.V. Pestrikov, R.A. Salimov, A.N. Skrinsky,
BINP, prospect Lavrenteva 11, 630090 Novosibirsk, Russia

Abstract

GSI has considered deep-inelastic electron-nucleon and electron-nucleus scattering at $\sqrt{s} = 10$ to 30 GeV/u as one of the options for the future development of the Laboratory. Therefore, a feasibility study was started for an electron-nucleus collider designed for high luminosity operation at $L = 1 \cdot 10^{33}$ cm^{-2}s^{-1} (e-p) and at $L = 4 \cdot 10^{30}$ cm^{-2}s^{-1} (e-U). In addition, longitudinal polarization of the colliding bunches was included. High luminosity operation in this intermediate energy range makes application of strong cooling for both the electron and the ion bunches absolutely necessary. We report on the main results of this feasibility study for such a collider, which was performed at BINP and GSI. As a consequence of the feasibility study, DESY, GSI, and the BINP have started further studies in the field of high energy electron cooling.

1 INTRODUCTION

The physical motivations for high luminosity electron-nucleon colliders which could operate in the range of $\sqrt{s} =$ 10 to 30 GeV/u are significant and prominent [1] (see, as an example, Fig. 1).

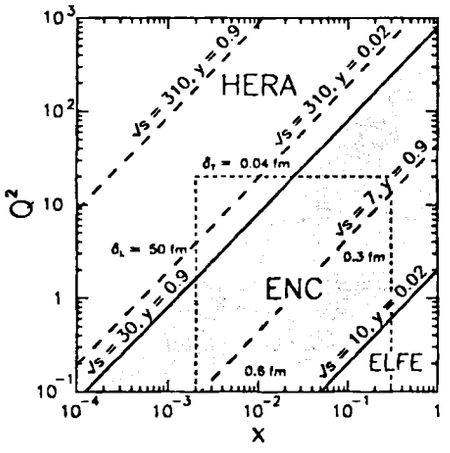

Figure 1: The kinematic range of the ENC in comparison to the HERA- and ELFE- energy regimes, respectively. $Q^2 = x \cdot y \cdot s$ is the square of the momentum transfer to a parton; x is the fraction of the momentum carried by the parton; $y = 1(0)$ corresponds to completely inelastic (elastic) scattering. The dashed box indicates the (x, Q^2)-range of particular importance for studying the transition from the perturbative to the non-perturbative QCD-regime.

A reasonable luminosity for such a collider should reach $L = 1 \cdot 10^{33}$ cm^{-2}s^{-1} per nucleon. The colliding bunches may have longitudinal polarization at the interaction points.

The preliminary study, which was performed at GSI and BINP during 1996–1998, has indicated that a construction of such a collider is quite feasible [2]. The currently envisioned operational modes should enable the collisions of electron against bare ion bunches from protons to ^{238}U. Two interaction points are foreseen.

The main interaction region (IR) will contain the detector solenoid ($\int Bdl = 5$ Tm) and two (up-stream and down-stream) spectrometer dipoles (DS; $\int Bdl =$ 1.7 Tm). The optical scheme of the main interaction region provides detailed observations of both large angle ($\theta > 10°$) and small angle ($\theta < 3°$) reaction products. For that reason, the optical elements in the main IR should be placed within the angular cone $3° < \theta < 10°$.

2 DESIGN CONCEPTS

The luminosity performance of the ENC is limited by the beam-beam instabilities. We assume that their strengths will be smaller if the lengths of colliding bunches will be close to the values of the β-functions at the interaction point (IP), while colliding bunches will have round cross sections at the IP, i.e. all 4 $\beta-$functions are the same. The luminosity of electron–nucleon collisions is then given by

$$L \simeq 0.75 A f_b \frac{N_i N_e}{2\pi\beta(\epsilon_i + \epsilon_e)} .$$

Here, subscripts i and e mark the values related to ion and electron bunches, $N_{i,e}$ are the numbers of particles in the bunches, $\epsilon_{i,e}$ are their emittances, β denotes the value of the β-function at the interaction point, A is the atomic number of the ion, and f_b the collision frequency of the bunches.

No unusual limitations on the ENC luminosity performance were detected due to collective interactions of the beams with their surrounding electrodes.

The strengths of the beam–beam instabilities are specified by two beam-beam parameters ($r_{e,p} = e^2/m_{e,p}c^2$):

$$\xi_e = \frac{N_i Z r_e}{4\pi\gamma_e\epsilon_i} \quad \text{and} \quad \xi_i = \frac{N_e Z r_p}{4\pi A\gamma_i\epsilon_e}.$$

The threshold values for ξ_e and ξ_i determine the maximum value of L. From the electron bunch side, the ENC does not present any special limitations, so that a ring average value of $\xi_e \simeq 0.05$ can be chosen as a threshold. The high threshold value for ξ_e is primarily due to synchrotron radiation damping pushing electrons towards the bunch core.

Relevant blow-up of the ion bunches should be suppressed by electron cooling. That and the desired values of the luminosity result in strong instabilities from the space charge fields of the bunches [2]. Those facts yield unique features of the beam–beam interactions which are specific for the ENC.

2.1 *Beam–beam instability*

Inspection of the betatron tune shifts in a space charge dominated ion beam indicated that better tune distributions are achieved, if the radii of the electron and ion bunches are set equal [2].

Threshold values of ξ_i were evaluated using multi-particle tracking simulations of the beam-beam interactions. Both cases (weak–strong and strong–strong beams) were studied. From the ion side, the typical turn-by-turn 6-dimensional transformation (map) included the following section maps:

- from the center of the first IP to the beginning of the cooling section;
- through the cooling section [3];
- from the cooling section to the second IP;
- through the second IP;
- to the center of the first IP;
- through the first IP.

The transformations were implemented using a linear map with the betatron phase advances corrected by the tune shifts due to the ion bunch space charge:

$$\Delta\nu_{x,z} = \frac{\Delta\nu_L}{\left(\frac{\epsilon_{x,z}+J_{x,z}}{\epsilon_0}\right)\sqrt{\frac{\epsilon_{z,x}+J_{z,x}}{\epsilon_0}}},$$

These expressions are quite realistic if the bunch cross section does not differ significantly from round (that fact is confirmed by simulations). Here, $\Delta\nu_L$ is the Laslett tune shift, ϵ_0 is the nominal bunch emittance, $\epsilon_{x,z}$ are the emittances calculated each turn using the ion coordinates at the IP, and $J_{x,z}$ are the action variables for betatron oscillations. The beam-beam kick was chosen to simulate expressions (for more detail see [2])

$$\delta(x',z') \propto \frac{-(x,z)}{\beta\epsilon_0 + x^2 + z^2}.$$

In our simulation we assumed round cross sections and envelopes of bunches, zero dispersion function and zero crossing angles at IP. The equilibrium ion bunch sizes without beam-beam interactions were set using their monochromatic instability (for more detail see [2], [4]). In the case of colliding bunches, in order to avoid the flip-flop blow-up of electron bunches, the required average velocity deviations of the cooling electron beam were set from the equilibrium bunch sizes corresponding to the threshold values of ξ_e. A usual slicing procedure was employed to simulate the bunch lengths. We took as an example the electron–U^{92}_{238} ENC operating mode, with $\sqrt{s} = 20$ GeV/u.

As a main result of these simulations, we may conclude that due to the collective interaction of the bunches the ion space charge results in a strong separation of the electron and ion bunch emittances if $\Delta\nu_L \simeq n_{\rm IP}\xi/2$ [5] ($n_{\rm IP}$ is the number of interaction points; see Fig. 2). This instability is not exactly the flip-flop phenomenon since the simulation has never shown the exchanges between the electron and ion bunch sizes. The bunch blow-ups were seen, when $\xi \geq 0.03$.

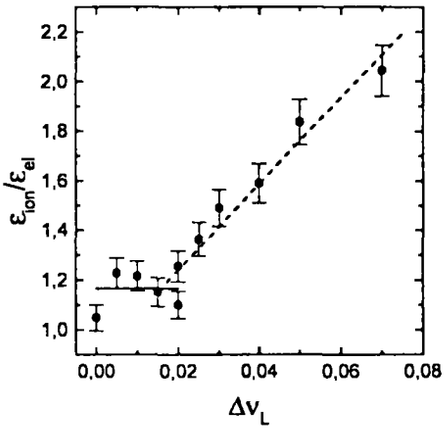

Figure 2: Dependence of the asymmetry in ion and electron bunch emittances on the ion bunch Laslett tune shift. Shown for one IP; $\xi = 0.05$, $\nu_x = \nu_z = 7.1$, $\nu_s = 0.003$.

2.2 *Optimum luminosity*

The high luminosity regimes in the ENC (with exception may be the high energy *e-p* mode) occur if the ion beam space charge fields dominate. Taking as a possible threshold value $\Delta\nu_L \simeq \xi_i$ (two IP), we find that for a given $\sqrt{s}$ the specific luminosity of the ENC reaches a maximum value

$$(L/N_e)_{\max} \simeq 0.75 f_b \left(\frac{A}{Z}\right)^{5/4} \frac{B^{1/4}\xi(\gamma_s/2)^{3/2}}{\beta r_p},$$

when

$$\gamma_i = (\gamma_i)_{\max} \simeq \left\{\frac{Z\gamma_s^2}{4AB}\right\}^{1/4}.$$

Here, $\gamma_s = \sqrt{s}/m_p c^2$, $B = \sigma_s\sqrt{2\pi}/\Pi$, where Π is the closed orbit path length. If either ion or electron energies deviate from the optimum value, the specific luminosity decreases according to

$$(L/N_e) = (L/N_e)_{\max}\begin{cases} \gamma_i^3/\gamma_{i,\max}^3, & \gamma_i \leq \gamma_{i,\max}, \\ \gamma_{i,\max}/\gamma_i, & \gamma_i \geq \gamma_{i,\max}. \end{cases}$$

2.3 *Parameter sets*

Described facts and equations were used for the calculations of the parameter sets enabling the luminosity of electron–nucleon collisions $L = 10^{33}$ cm^{-2}s^{-1} in the energy range $\sqrt{s} = 10$ to 30 GeV/u. In our estimations we considered as limiting cases the *e-p* and *e-U* operational modes of the ENC. General parameters of the ion and electron rings of the ENC for these estimations are

listed in Table 1. For particles with the optimum energies, the magnetic rigidity of the electron ring does not exceed 30 Tm, while that of the ion ring should be in the range $(BR)_i \leq 100$ Tm for the e-p mode of the ENC and in the range $(BR)_i = 100$ to 200 Tm for the e-ion mode.

Table 1: General parameters for the ion and electron rings of the ENC.

Closed orbit perimeter,	km	1.4
Collision frequency,	MHz	60
$\chi = \epsilon_e/\epsilon_i$		1
Curvature radius in bending magnets,	m	60
β−functions at IP,	cm	10
Rms bunch length,	cm	10
Average β−functions in the arc,	m	12
Average dispersion function D_x in the arc,	m	1.6
Momentum compaction factor		0.006
β−function in the cooling section,	m	200
Length of the cooling region,	m	50
Transverse cooling electron temperature (cathode temp.),	eV	0.1
Longitudinal magnetic field in the cooling region,	T	0.5
$\xi_e = \xi_i$		0.05

Table 2: Parameter sets for the e-p and e-U colliders, calculated assuming a luminosity 10^{33} cm^{-2}s^{-1} per nucleon, $(\Delta\nu_L)_{th} = \xi_i$ (two IP), and $\xi_i = \xi_e = 0.05$, 50 kV RF-voltage in the ion ring.

Mode		e-p			e-U (bare)		
$\sqrt{s}$,	GeV/u	10	20	30	10	20	30
Specific $L/10^{21}$,	1/cm^{2}s	2.3	6.5	12	7.6	21.4	39.4
Parameters		Ion Ring					
Bunch intensity,	10^9	36	26	21	.075	.053	.043
Beam current,	mA	350	250	200	66.5	47	38.4
Energy,	Gev/u	17.2	24.3	29.8	13.57	19.19	23.51
Emittance,	nm	57.3	14.3	6.4	8.6	2.1	1
$(Z/n)_{th}$,	Ohm	1.8	3.3	4.5	11.5	23	33
IBS growth time,	s	6.5	1.9	1	.06	.014	.07
Cooling time,	ms	700	170	76	22.45	5.5	2.6
Radiative recombination lifetime,	h	87	61	50	0.21	0.15	0.12
Parameters		Electron Ring					
Bunch intensity,	10^{10}	43.	15.	8.3	13.2	4.7	2.5
Beam current,	A	4.2	1.5	0.8	1.27	0.45	0.24
Energy,	GeV	1.45	4.1	7.55	1.8	5.2	9.6
Emittance,	nm	57.3	14.3	6.4	8.56	2.14	0.95
Energy loss/turn,	MeV	0.007	0.43	4.9	0.02	1.1	12.6
RF-Power,	MW	0.03	0.6	4	0.02	0.5	3.0
$(Z/n)_{th}$,	Ohm	0.03	1.0	8.5	0.16	6	51
Bremsstrahlung lifetime,	h	50	22	15	0.5	0.2	0.14

In Table 2 one can see the very short lifetimes of the bunches for e-U mode. For that reason it is necessary to reinject frequently. Analysis shows this can be done [2].

3 ELECTRON COOLING DEVICE

The main goal for the cooling system of the ENC is the suppression of bunch blow-ups due to the beam–beam and space charge instabilities. As is seen from Table 2, for the ion bunches the desired cooling rates exceed about 10 times the emittance growth rates due to intrabeam scattering. In practice, such short cooling times can be achieved only in the case where magnetized cooling predominates. The required parameters of the electron beam to ensure such cooling times are listed in Table 3. Up to now, most studies

Table 3: Parameter set requirements for the electron cooling device.

Ions		Protons			Bare U		
$\sqrt{s}$,	GeV/u	10	20	30	10	20	30
Cooling time,	ms	700	170	76	22.45	5.5	2.6
Beam density/10^9,	1/cm^3	4	11	21	.056	.16	.3
Beam current,	A	14	9.9	8	.03	.02	.017
Rms beam radius,	cm	0.3	0.17	0.11	0.13	0.06	0.04
Current density,	A/cm^2	19.4	55	101	0.27	0.76	1.4
$B_\perp/B_{sol}$,	μrad	17	8.4	5.6	6.5	3.2	2.2
$T_\parallel = e^2(n_e/\gamma_i)^{1/3}$,	K	1	1.2	1.4	0.24	0.3	0.36

focused on employing a DC-acceleration facility as a cooling device. The schematic layout and general parameters of such a cooling device are shown in Fig. 3.

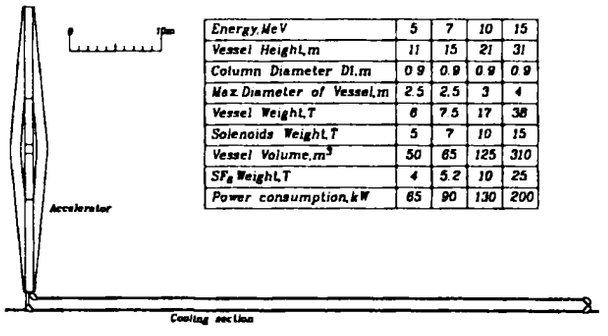

Figure 3: General layout of a DC-cooling facility. Electron beam parameters correspond to the $\sqrt{s}$−value in Table 2.

An additional possibility is to generate the cooling beam using a linac. Preliminary estimations [2] have shown that this is feasible for the ENC energy range.

4 LATTICE DESIGN

The lattice design includes the following features:

- low emittance arc lattices;
- main interaction region;
- cooling region straight section;
- synchronization of ion and electron revolution frequencies;
- chromatic corrections and dynamic aperture;
- polarization control;
- injection chain.

The results obtained for some of these problems are presented below.

4.1 *Interaction region*

The lattice of the main interaction region (IR; see Fig. 4 and Table 4) provides the following options:

- head-on collisions;
- equal and small β–functions ($\approx$ 10 cm) at the interaction point (IP);
- electron–ion beam separation at the first parasitic IP (not less than (5 to 7)$\sigma_\perp$);
- longitudinal polarization of the bunches at IP;
- the required optical elements inside the detector should be placed within the cone $3° \leq \alpha \leq 10°$.

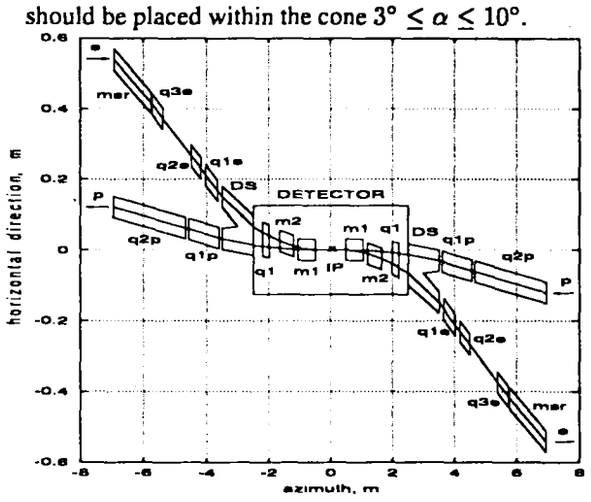

Figure 4: Layout of the interaction region around the IP for both rings.

Table 4: Parameters of the elements around IP for the ENC with $\beta^* = 10$ cm (a – combined magnet, b – shifted lens, c – dipole magnet of the spectrometer).

element inside detector		m1 a	m2 a	q1 b	DS c
dist. from IP,	cm	48.92	119.43	198.99	250
L,	cm	56.72	46.02	20.78	100
α (for e^-),	mrad	23.82	18.50	87.60	68
B,	T	1.0499	1.0049	1.035	17
G,	T/cm	0.275	0.109	−.2360	–
beam separation data					
place		after detector		after DS	
β_x ,	m	19.85		25.10	
σ_x ,	cm	$3.01 \cdot 10^{-2}$		$3.40 \cdot 10^{-2}$	
beam separation	cm	5.16		11.96	
beam separation,	σ_x	170		3500	

The chosen scheme for the IR eliminates the parasitic IP for colliding bunches (immediately outside the detector).

4.2 *Adjustment system*

Colliding electron and ion bunches must have identical revolution frequencies. Since electrons are ultra-relativistic, their revolution frequency is practically constant. On the contrary, the ions in the ENC are only weakly relativistic. For that reason, in the energy range of the ENC the ion revolution frequency and hence the circumference of the ion orbit may vary significantly (Fig. 5). Adjustment of the closed ion orbit circumference with increasing ion energy can be achieved using special orbit bumps (Fig. 6). Each bump provides the same bending angle as the replaced cells. Table 5 and Fig. 7 show that the scheme with 8 orbit bumps enables the lowest required radial displacement of the ion orbit. In this case the ENC operation in the energy range from 25 GeV to 30 GeV can be carried out using magnets with large radial apertures.

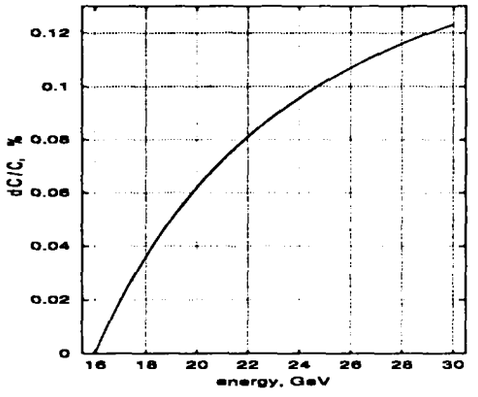

Figure 5: Dependence of the required relative adjustment of the ion closed orbit circumference on the ion energy. In this figure the reference energy is $E_{ref} = 16$ GeV.

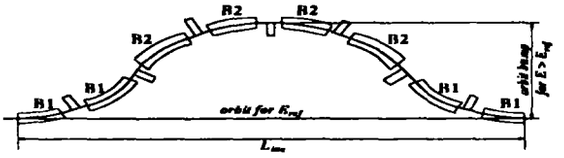

Figure 6: The principle scheme of the orbit bump element adjustment system.

Table 5: Characteristics of the adjustment systems for $E_{ref} = 16$ GeV and $\Pi = 1400$ m.

E_{proton}, GeV		25			30		
$\Delta\Pi$,	m	1.4229292			1.7243386		
Total N_{bump}		1	4	8	1	4	8
L_B,	m	3.5					
L_{drift},	m	3.20	3.05	2.02	3.25	3.062	2.03
L_{ins},	m	50.42	49.36	42.18	50.72	49.43	41.24
B_{B1},	T	2.181	.161	0.033	3.129	.420	.130
B_{B2},	T	4.478	2.458	1.935	5.884	3.176	2.493
Total N_{bend},	m	8	32	64	8	32	64
Total N_{lens},	m	7	28	56	8	28	56
Orbit bump,	m	3.592	1.301	.805	4.087	1.519	.938
ΔR for the orbit bumps from 25 GeV till 30 GeV							
Total N_{bump}		1		4		8	
ΔR,	cm	49.5		21.8		13.3	

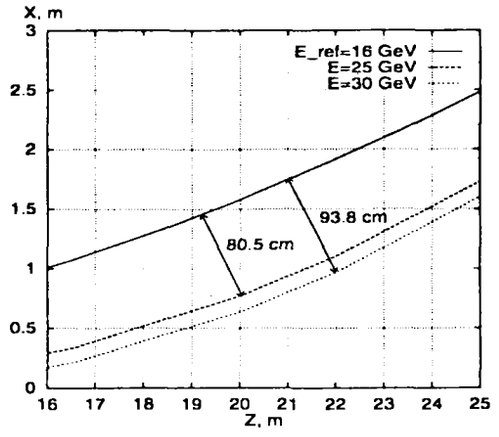

Figure 7: Orbit bumps for different energies in a quarter of the ring (with large magnification).

4.3 *Polarization control*

For electron-proton (light ion) operational ENC modes, the radiation polarization time of electrons can be made less than 30 min using special wiggler magnets [2] (see Table 6). Two wigglers provide the required polarization time for $E = 7.5$ GeV, three wigglers for $E = 4$ GeV, and five wigglers are necessary for $E = 3$ GeV. For operation

Table 6: Wiggler characteristics.

The basic pole,	T · cm	7.097 · 12
Compensating poles,	T · cm	2 × 1.581 · 35
Magnet length,	cm	82
$< \|B\|^3 >$ [1]	T^3	0.0375
$\oint B^2 ds$ [1]	T^2·cm	780
$\oint \|B\|^3 ds$ [1]	T^3·cm	$4.5 \cdot 10^3$
Degree of polarization	%	81.2

[1] If one considers options for a different beam energy, the wiggler field H does not change.

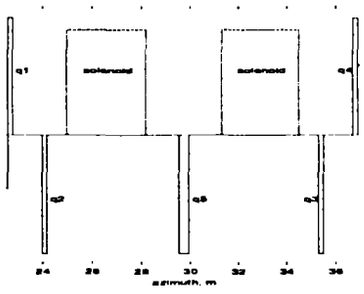

Figure 8: Solenoid spin rotator insertion (e–ring).

at an energy of 1.6 GeV and for electron–heavy ion ENC modes, polarized electrons should be produced using a special source. The longitudinal polarization of electrons at the IP is obtained using two standard spin rotators. Each of them includes two solenoids, two pairs of skew quadrupole lenses, and one standard quadrupole lens which is placed between the solenoids (see Table 7 and Fig. 8). In the chosen scheme, the vertical-horizontal coupling of the particle oscillations is localized in the rotator.

Both the acceleration of the polarized protons and production of the longitudinal polarization at the interaction point can be performed using "continuous" Siberian snakes and rotators, which are manufactured using helical magnets [6]. Although the field integral ($\int Bds$) is higher when helical magnets are used, the power capacity of such a snake ($\sim \int B^2 dV$) is lower due to smaller magnet apertures. The required parameters of the snakes (see Table 8 and Ref. [2]) indicate that their manufacturing and operation are feasible.

Table 7: Main parameters of the solenoid spin rotator.

element	name	number	L, m	G, T/cm	sign(α_{tilt})
lenses	q1	2	0.2	.3423	−, +
	q2	2	0.2	−.3447	−, +
	q5	1	0.4	−.2972	no
solenoid		2	3.2	$B = 6.129$ T	

Table 8: Parameters of the snakes for acceleration of polarized protons (accel.) and providing longitudinal polarization (long.p.) at the IP.

type of snake	number of magnets	$\int Bdl$, Tm	ion orbit deviation (cm) different energies (GeV) 30	25	16
A (accel.)	4	25.5	2.6	3.1	4.8
B (accel.)	4	24.5	2.0	2.4	3.8
C (accel.)	4	30.9	2.0	2.4	3.7
C (long.p.)	4	22.9	1.7	2.0	3.2
D (long.p.)	3	19.9	2.2	2.7	4.2

5 CONCLUSIONS

This study shows that the construction of an electron-nucleon collider for the energy range $\sqrt{s} = 10$ to 30 GeV/u and with a luminosity of $L = 1 \times 10^{33}$ cm^{-2}s^{-1} per nucleon is feasible provided that the ion bunches can be cooled sufficiently fast. The required cooling devices (both DC and RF) may demand more research and development.

More beam dynamics studies are needed to understand performance limitations due to ion bunch space charge effects.

In the course of producing this Design Study, we had numerous valuable comments from the members of Working Groups I and VII on Long Term GSI Perspectives. These comments are kindly acknowledged.

6 REFERENCES

[1] Deep-inelastic electron–nucleon/nucleus scattering at $\sqrt{s} =$ 10 to 30 GeV (Summary of the Working Group 1).

[2] Conceptual Design Study of the GSI Electron-Nucleon Collider. http:/ /www.gsi.de/ ~struck/ concepts.html, GSI 1998.

[3] D.V. Pestrikov. NIM, A412 (1998) 288.

[4] V.V. Parkhomchuk, A.N. Skrinsky. Rep. on Progr. in Phys., 54 (1991) 919.

[5] D.V. Pestrikov. NIM, A412 (1998) 278.

[6] V.I. Ptitsyn, Yu.M. Shatunov. Brookhaven National Laboratory, BNL-52453,1994 (Third Workshop on siberian snakes and spin rotators, Sept. 1994).